# Breakthroughs in Spatial Biology: AGBT 2025 Highlights

AGBT 2025 was a whirlwind of innovation and excitement. Our Morning Buzz Sessions provided deep dives into the latest in spatial biology each day, while our Brews with Bruker gatherings served up lively conversation over craft brews. We also hosted a Silver Sponsor Workshop, where experts led in-depth discussions across all Bruker platforms. Whether you joined us in person or are catching up from afar, check out the posters we presented and stay caught up on our latest scientific breakthroughs.

## Streamlining Imaging-Based Spatial Biology with EpicIF – A Universal Signal Removal Strategy

This poster demonstrates how EpicIF™ technology enables flexible, high-plex immunofluorescence on the same tissue section, removing existing fluorescence signals after each imaging cycle to streamline multi-omic assays. By coupling iterative protein immunofluorescence, RNA-FISH, and an *in situ* proximity ligation assay (isPLA) on a single FFPE slide, we pinpoint not only protein and transcript levels but also direct protein–protein interactions (PD-1/PD-L1). We illustrate this with an invasive ductal carcinoma sample, profiling tumor and immune cells (including tertiary lymphoid structures) to reveal nuanced immunoregulatory processes in the tumor microenvironment.

Read the Full Poster

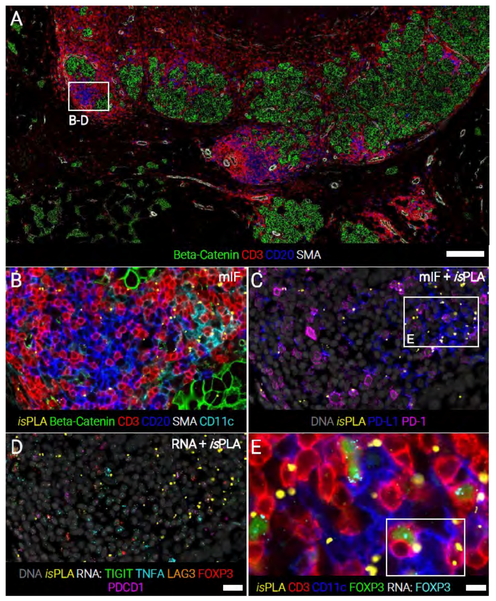


## CosMx SMI Spatially Resolved Whole Transcriptome in FFPE Tissue – A Paradigm Shift for Tissue Analysis

This poster showcases how CosMx® Whole Transcriptome (WTX) technology overcomes the limitations of tissue dissociation and single-cell capture in conventional single-cell RNA sequencing (scRNA-seq). By profiling adjacent FFPE sections in parallel with droplet-based scRNA-seq, we demonstrate that CosMx WTX can detect a highly comparable set of genes while fully preserving spatial context. Additionally, we capture extremely rare cell types commonly lost in dissociation-based methods. We also highlight the workflow's exceptional throughput, recovering hundreds of thousands of cells and delivering more comprehensive data than scRNA-seq alone.

Read the Full Poster

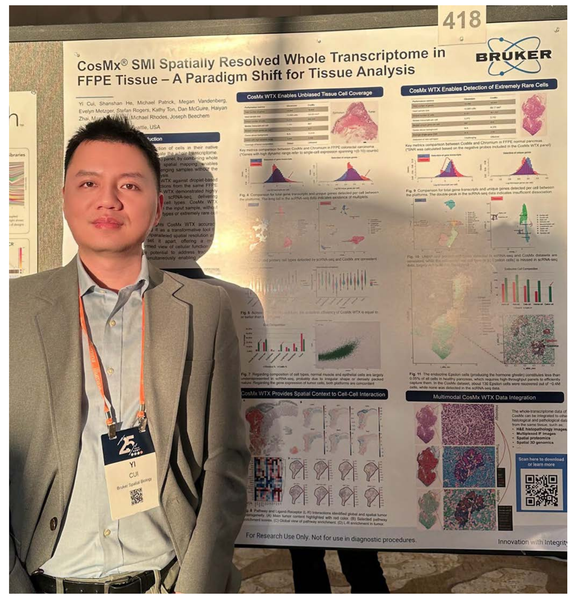


## Cell Segmentation for Complex Neural Cell Morphologies & CosMx Whole Transcriptomics Brain Imaging

This poster introduces a new cell segmentation approach tailored to the intricate shapes found in brain tissue, which is especially useful when performing high-coverage spatial research with the CosMx Whole Transcriptome panel. By training a specialized neural network on diverse neuronal cell types and employing a "high-recovery" post-processing method, we show how our pipeline captures challenging star-like and elongated cells that more generic models often miss. In practical tests on FFPE human brain samples, the improved segmentation recovers more transcripts per cell, removes "ghost" cells, and yields higher-quality data for downstream analyses.

Read the Full Poster

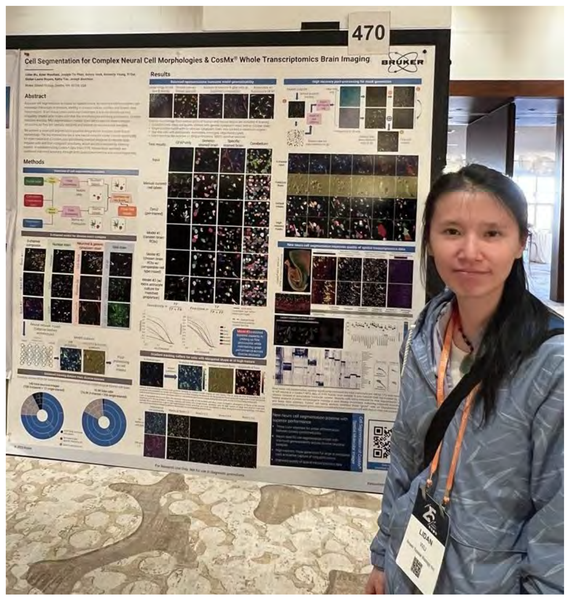


## InSituDiff: Disease-Driven Changes in Cellular Neighborhoods as a Window into Spatial Transcriptomics

This poster introduces InSituDiff, a new computational framework for identifying how disease or other perturbations reshape cellular neighborhoods based on CosMx SMI spatial transcriptomics data. By comparing neighborhoods in infected or diseased tissues to their closest match in healthy controls, InSituDiff builds a "perturbation matrix" for each gene, highlighting which genes (and which areas) are most changed. We then employ standard single-cell analytics (clustering, network analysis, etc.) on these perturbation profiles, revealing spatially correlated gene modules and distinct "perturbation domains."

Read the Full Poster

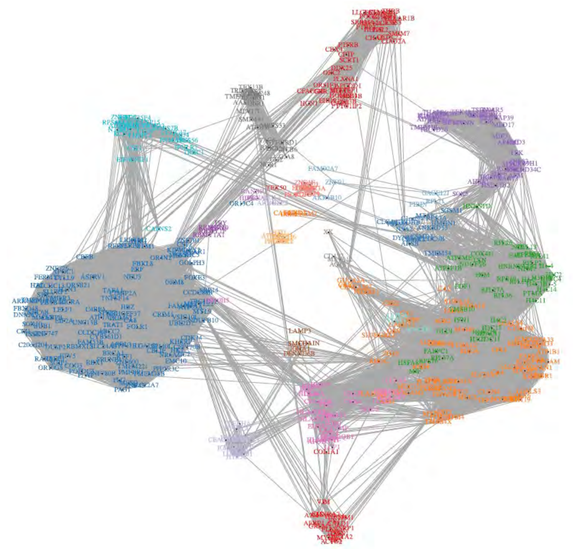

## Connecting Form and Function: Mapping Microglial Spatial Biology in a Mouse Model of Acute and Chronic Ischemic Stroke

This poster highlights how CosMx SMI can map microglial form and function in the mouse brain following ischemic stroke. By combining single-cell proteomics with morphological analysis, our collaborative partnership with University of Arizona researchers captures how microglia transition from surveillance to injury-response states and reveals distinct gene expression patterns in infarcted versus healthy regions. Notably, we demonstrate that proteins like TMEM119, Cathepsin B, and DAP12 change in both intensity and spatial distribution as you move away from the infarct core, indicating functional heterogeneity across brain regions.

Read the Full Poster

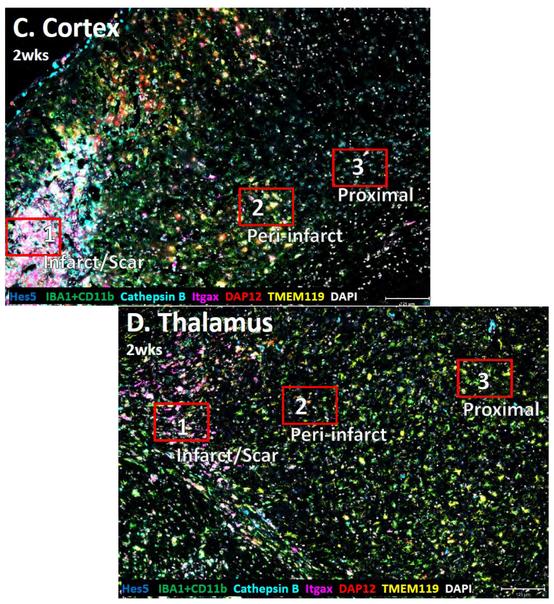


## Expanding the Limits of Spatial Biology: Comprehensive Integrated Technologies for Spatial Multiomics

Our Silver Sponsor Workshop is now available to stream on demand! Catch up on all of our technology announcements:

- 3D genome exploration with the **new** PaintScape™ platform
- Pathways-first biology with the world's only unbiased, single-cell whole transcriptome solution using CosMx® SMI
- Unparalleled discovery multiomics with GeoMx® WTA + over 1000 proteins
- Improvements in data and image quality with the PowerOMX™ engine for the CellScape platform
- New customer success programs

Watch On-Demand

AGBT 2025 POSTER #411

# Streamlining imaging-based Spatial Biology with EpicIF - a universal signal removal strategy.

**Oliver Braubach**[1], **Jannik Boog**[1], **Thore Böttke**[1] and **Arne Christians**[1], Bruker Spatial Biology, 4340 Duncan Street, Saint Louis, MO 63110, USA.

## Streamlining imaging-based Spatial Biology

Imaging-based spatial biology is an iterative process of biomarker labeling, imaging, and signal removal. Removing fluorescence signals is central to the experiment and pursued in various ways, including photobleaching, antibody stripping, and antibody barcoding. Each method has limitations and introduces unique challenges to the realization of multiplex assays.

We developed **E**nhanced **p**hotobleaching **i**n **c**yclic **i**mmunof**l**uorescence (**EpicIF**™) to allow quick, gentle, and complete removal of photostable fluorophores *in situ,* and to streamline the development of multi-omic assays on the CellScape™ platform.

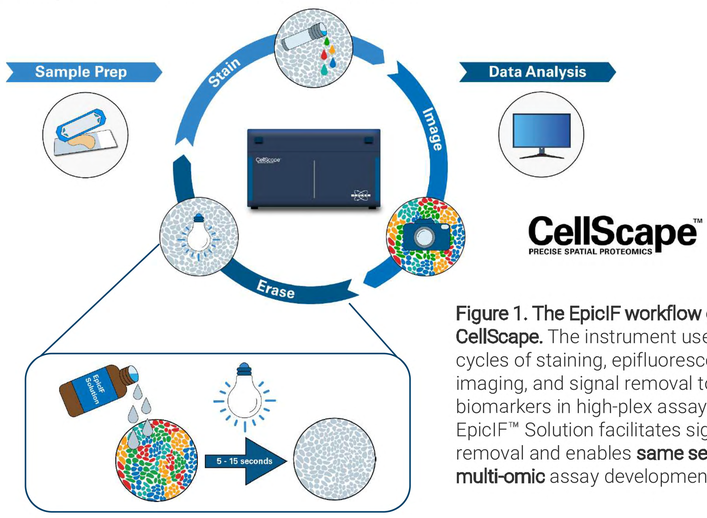


**Figure 1. The EpicIF workflow on the CellScape.** The instrument uses cycles of staining, epifluorescence imaging, and signal removal to detect biomarkers in high-plex assays. EpicIF™ Solution facilitates signal removal and enables **same section multi-omic** assay development.

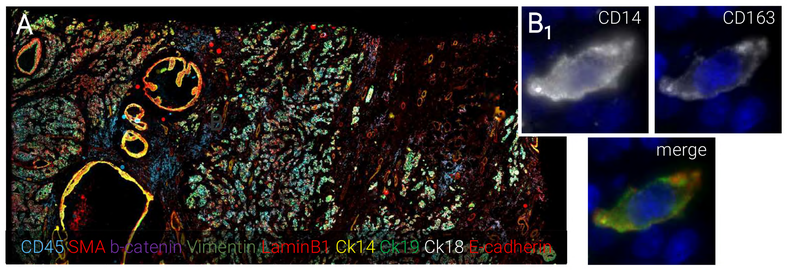


**Figure 2: 48-plex FFPE Invasive Ductal Carcinoma (IDC)**. A 12-cycle multiplex immuno-fluorescence (mIF) stain with EpicIF technology. **(A)** Overview showing marker-specific staining patterns. **($B_{1-2}$)** A cross-correlation analysis over staining cycles confirms complete signal removal through successive cycles. Markers with the same fluorophore are outlined with boxes. Higher correlations between certain markers (r=0.71 for CD14/CD163) were confirmed to be due to biological spatial colocalization rather than incomplete signal removal by EpicIF ($B_1$). Co-localizing markers have distinct expression patterns (e.g. CD14 and CD163).

## Same section multi-omic assays enabled by EpicIF

Since EpicIF requires no chemical modifications of targeting probes or experimental tissues, it presents an opportunity to integrate multi-omic analyte detection in same tissue sections. To this end, we integrated mIF with hybridization chain reaction RNA-FISH (HCR RNA-FISH) on single tissue sections.

### Same section multi-omic immune profiling

| Cycle | 488 | 532 | 594 | 647 | Cycle | 488 | 532 | 594 | 647 |
|---|---|---|---|---|---|---|---|---|---|
| 1 (RNA) | CD3E | CD274 | TNFA | TIGIT | 7 | CD11c | Ki-67 | CD8a | CD4 |
| 2 (RNA) | KRT19 | PDCD1 | FOXP3 | LAG3 | 8 | Gran B | CD34 | CD68 | CD138 |
| 3 (RNA) | MALAT1 | CD8A | IL6 | CTLA4 | 9 | LAG-3 | CD31 | CK19 | ER |
| 4 | DNA | | | | 10 | CD16 | open | CD14 | CD20 |
| 5 | CD3 | CD45 | CD274 | HLA-DR | 11 | HER2 | open | FOXP3 | CD66b |
| 6 | CD279 | Vimentin | CD163 | CD123 | 12 | p53 | SMA | B-Cat | PR |

**Table 1**. Assay layout by cycle and channel. RNA-FISH was performed first, followed by DNA and mIF stains. Complete signal removal between cycles was accomplished with EpicIF and filtered photobleaching.

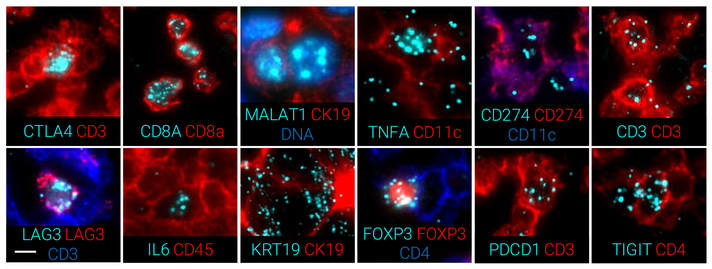


**Figure 3**. High dynamic range imaging coupled with the excellent resolution of the CellScape allows precise localization and quantification of RNA-FISH signals. The RNA-FISH signals are shown in cyan; reference antibody stains are shown in red and blue. The scalebar represents 5 µm and applies to all images.

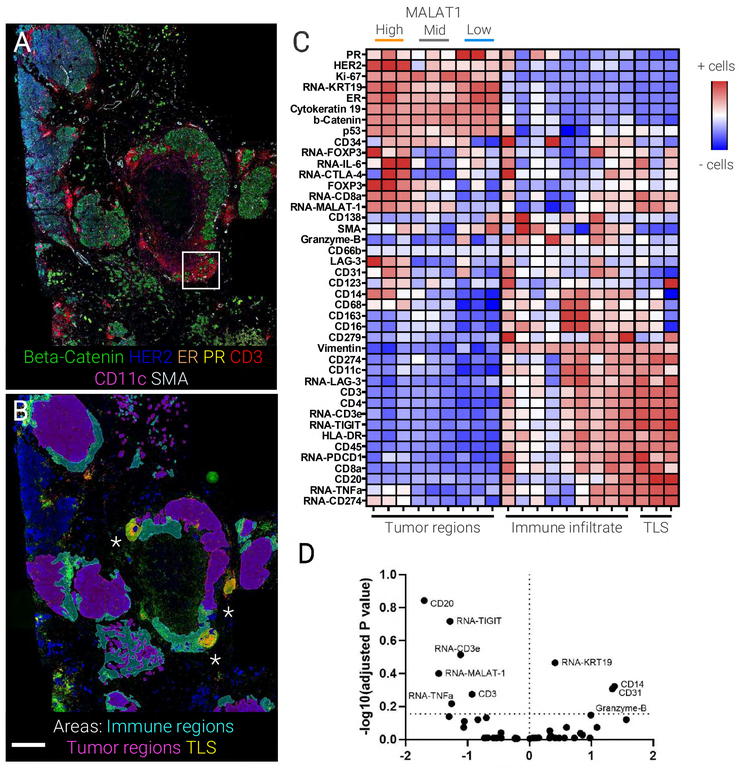


**Figure 4**. (**A**) Multi-omic staining of an IDC, segmented into tumor and TiME regions (**B**) based on expression of key breast cancer biomarkers HER2, ER and PR, as well as immune markers. Putative tertiary lymphoid structures (TLS) are marked with asterisks. The scalebar represents 800µm. (**C**) Heatmap showing cell-based quantification for RNA and protein biomarker signals in IDC (**B**). (**D**) The TLS regions show higher expression of certain immune and inflammatory markers compared to the immune infiltrate.

## A same section tri-omic assay enabled by EpicIF

Building on the successful integration of mIF and RNA-FISH assays, we next devised a workflow that combines mIF, RNA-FISH and an *in situ* proximity ligation assay (*is*PLA), to additionally detect protein-protein interactions between the PD-1 receptor and its ligand PD-L1.

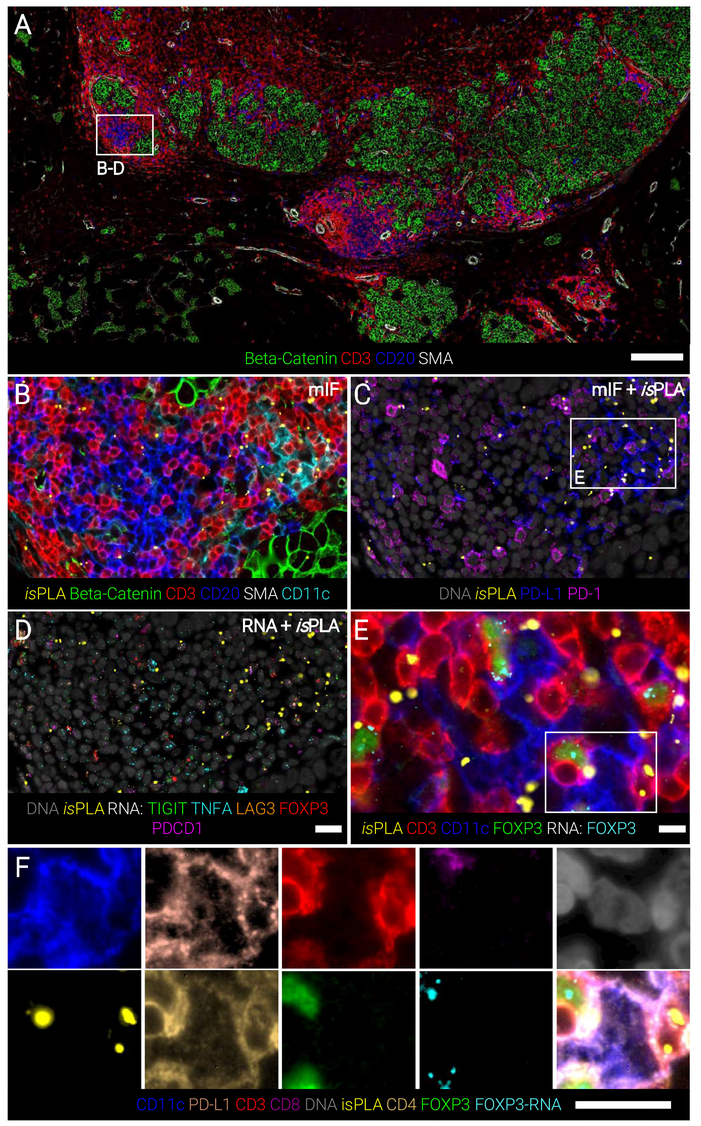


**Figure 5**. The combination of proteomic, transcriptomic and interactomic data on the same section enables comprehensive mapping of immune regulatory processes in the TiME. **A.** Overview of an IDC sample with areas of lymphocyte aggregation, indicative of TLS formation. (**B**, **C**) Aggregating B-cells in the center of the putative TLS. CD11c+ PD-L1+ follicular dendritic cells (FDCs) and T-cells engage in immune regulation via PD-1/PD-L1 interaction, signified by PD-1/PD-L1 *is*PLA signal (yellow). (**D**) RNA FISH staining allows detection of immune regulatory factors in the TLS that are difficult to detect by antibody staining (e.g. secreted cytokine TNFA); TNFA expression is elevated in the B-cell enriched TLS. **E**-**F.** Precise localization of mIF, FISH and isPLA signals illustrate an immune regulatory process, where regulate the activity of helper T-cells.
Scale bar represents (**A**) 250 µm, (**B**-**D**) 20 µm, (**E**, **F**) 5 µm.

## Streamlining Spatial Biology

- EpicIF on CellScape allows for fast and modular multiplexing, regardless of which biomarker assay is used.
- EpicIF streamlines the development and rapid deployment of same section multi-omic assays.



For Research Use Only. Not for use in diagnostic procedures.

Innovation with Integrity

# CosMx® SMI Spatially Resolved Whole Transcriptome in FFPE Tissue – A Paradigm Shift for Tissue Analysis

Yi Cui, Shanshan He, Michael Patrick, Megan Vandenberg, Evelyn Metzger, Stefan Rogers, Kathy Ton, Dan McGuire, Haiyan Zhai, Margaret Hoang, Michael Rhodes, Joseph Beechem

Bruker Spatial Biology, Seattle, USA

## Introduction

Spatial technologies allow the dissection of cells in their native context but lacked the ability to interrogate the whole transcriptome. The CosMx® Whole Transcriptome (WTX) panel, by combining whole transcriptome profiling with nanometer spatial mapping, enables direct analysis and visualization in challenging samples without the limitations of tissue dissociation and cell lysis.

In this study, we benchmarked CosMx WTX against droplet-based scRNA-seq. By processing adjacent sections from the same FFPE block tissue on both techniques, CosMx WTX demonstrated highly comparable detection efficiency with scRNA-seq, delivering consistent cell identification for major cell types. CosMx WTX produced data on over 95% of the cells in the input sample, without dissociative loss of irregularly shaped cell types or extremely rare cell types typically seen in scRNA-seq.

Our cross-platform evaluation highlights CosMx WTX accuracy, scalability, and versatility, positioning it as a transformative tool for various research applications. Its unparalleled spatial resolution and whole transcriptome coverage set it apart, offering a more comprehensive and spatially informed view of cellular function and tissue structure, which has the potential to address traditional scRNA-seq applications, while simultaneously enabling biological insights with spatial context.

## CosMx WTX panel Design

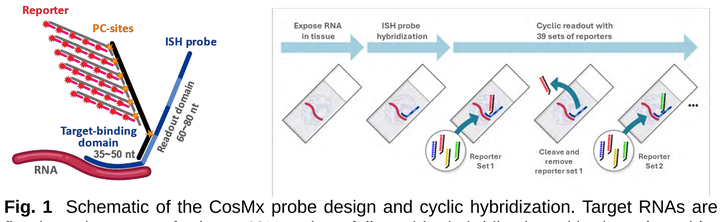


**Fig. 1** Schematic of the CosMx probe design and cyclic hybridization. Target RNAs are first bound to a set of primary ISH probes, followed by hybridization with photocleavable, fluorescent secondary “reporters”. The “hybridization-imaging-cleavage-rehybridization” is programed to barcode 18,935 gene targets in human transcriptome.

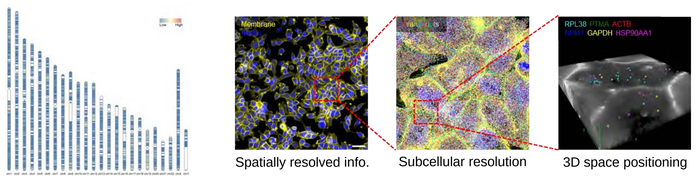


**Fig. 2** The CosMx WTX panel enables full coverage of human protein-coding genes (genomic loci as shown in the T2T karyotype density diagram), and visualization in spatial context with subcellular resolution and 3D localization capability.

## Experimental Design

| | | | | | |
|---|---|---|---|---|---|
| Chromium | Deparaffinization → | Tissue dissociation → | Barcoding → | Library preparation → | NGS |
| Sample size | 2 x 25um sections | 100K-1M cells | 10,000s of cells | 60-70% barcoded cells | |
| CosMx | Deparaffinization → | Antigen retrieval → | Tissue permeabilization → | ISH & IF → | Imaging |
| Sample size | 1 x 5um section | 500K-1M cells | 500K-1M cells | 500K-1M cells | |

Workflow summary of benchmarking CosMx WTX panel performance against the droplet based scRNA-seq technique (using Miltenyi Biotec’s FFPE Tissue Dissociation Kit for RNA Profiling and 10x Chromium Flex Gene Expression). The brief sample input/yield numbers are based on matching the cost on each platform. The Chromium run and scRNA-sequencing was carried out by Azenta Inc. a formally certified service provider.

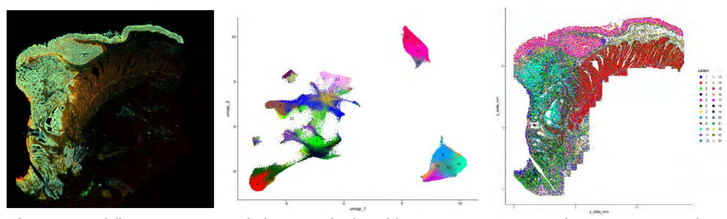

**Fig. 3** Workflow summary of data analysis with CosMx WTX panel. Gene expression matrix went through Log1P normalization, z-score transformation, principal component analysis (PCA) and Uniform Manifold Approximation and Projection (UMAP). Then unsupervised Leiden clustering was performed, followed by spatial mapping of cell clusters to tissue space. For comparison with scRNA-seq, obtained Leiden clusters were annotated based on marker gene expression and identity-matched between the platforms.

## CosMx WTX Enables Unbiased Tissue Cell Coverage

| Performance metrics | Chromium | CosMx |
|---|---|---|
| Total number of genes | 18,082 | 18,935 |
| Input sample size | 10,000 cells | 103.63 mm$^2$ |
| Output number of cells | 6,275 | 493,929 |
| Median transcripts per cell | 1,151 | 967 |
| Median unique genes per cell | 774 | 627 |
| Genes above background | N.A. | 13,918 |
| Genes with high dynamic range | 3,349 | 5,896 |
| Coverage of tissue composition | Biased | Unbiased |

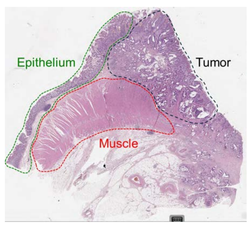


Key metrics comparison between CosMx and Chromium in FFPE colorectal carcinoma (*Genes with high dynamic range refer to single-cell expression spanning >(0-10) counts)

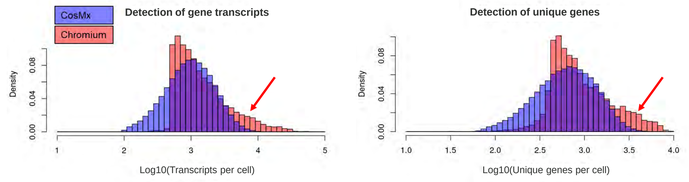


**Fig. 4** Comparison for total gene transcripts and unique genes detected per cell between the platforms. The long tail in the scRNA-seq data indicates existence of multiplets.

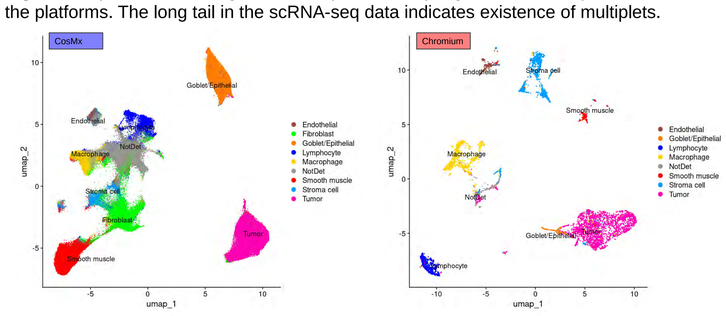


**Fig. 5** UMAP and primary cell types detected by scRNA-seq and CosMx are consistent

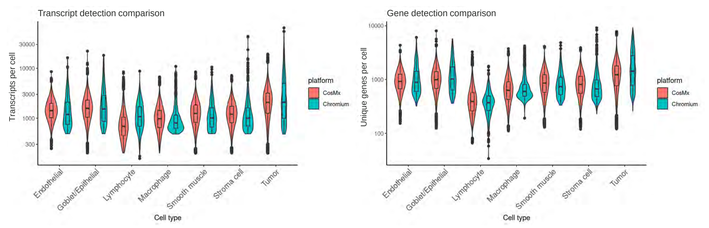


**Fig. 6** Across each primary cell type, the detection efficiency of CosMx WTX is equal to, or better than scRNA-seq

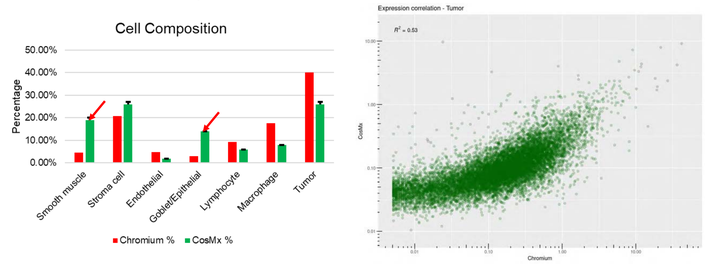


**Fig. 7** Regarding composition of cell types, normal muscle and epithelial cells are largely underrepresented in scRNA-seq, probably due to irregular shape or densely packed nature. Regarding the gene expression of tumor cells, both platforms are concordant

## CosMx WTX Provides Spatial Context to Cell-Cell Interaction

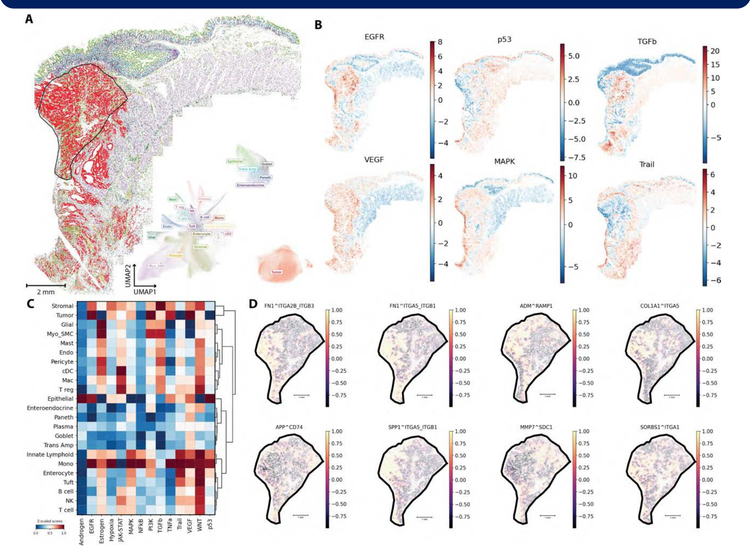


**Fig. 8** Pathway and Ligand-Receptor (L-R) Interactions identified global and spatial tumor heterogeneity. (A) Main tumor content highlighted with red color. (B) Selected pathway enrichment scores. (C) Global view of pathway enrichment. (D) L-R enrichment in tumor.

## CosMx WTX Enables Detection of Extremely Rare Cells

| Performance metrics | Chromium | CosMx |
|---|---|---|
| Total number of genes | 18,082 | 18,935 |
| Input sample size | 10,000 cells | 69.17 mm$^2$ |
| Output number of cells | 8,551 | 401,797 |
| Median transcripts per cell | 3,373 | 2,112 |
| Median unique gene per cell | 697 | 839 |
| Genes above background | N.A. | 8,370 |
| Average single-gene SNR | N.A. | 9.93 |
| Detection of rare cell types | Challenging | Effective |

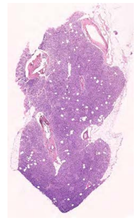

Key metrics comparison between CosMx and Chromium in FFPE normal pancreas (*SNR was calculated based on the negative probes included in the CosMx WTX panel)

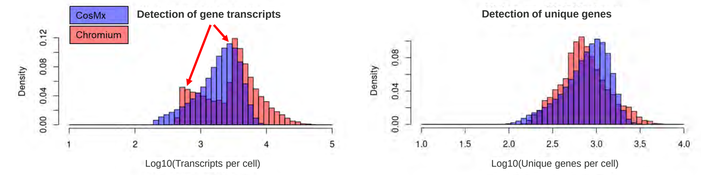


**Fig. 9** Comparison for total gene transcripts and unique genes detected per cell between the platforms. The double-peak in the scRNA-seq data indicates insufficient dissociation.

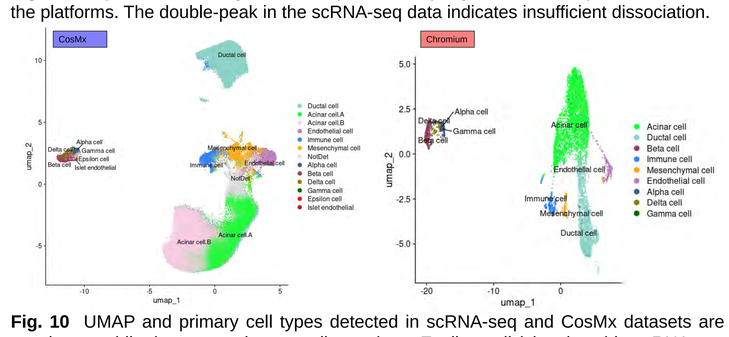


**Fig. 10** UMAP and primary cell types detected in scRNA-seq and CosMx datasets are consistent, while the extremely rare cell type (e.g., Epsilon cells) is missed in scRNA-seq data, largely due to its low throughput

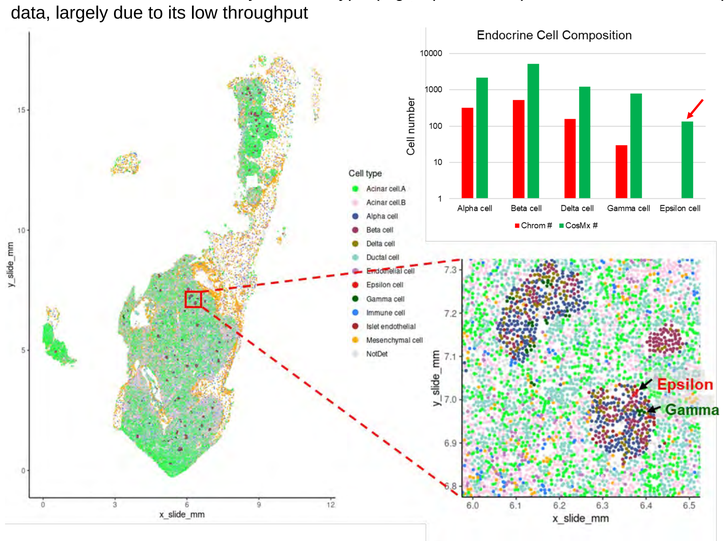


**Fig. 11** The endocrine Epsilon cells (producing the hormone ghrelin) constitutes less than 0.05% of all cells in healthy pancreas, which requires high-throughput panels to efficiently capture them. In the CosMx dataset, about 130 Epsilon cells were recovered out of ~0.4M cells, while none was detected in the scRNA-seq data.

## Multimodal CosMx WTX Data Integration

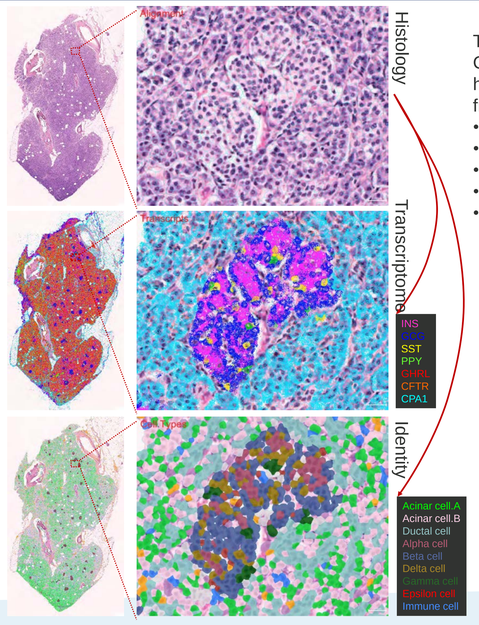


The whole-transcriptome data of CosMx can be integrated to other histological and pathological data from the same tissue, such as:

- **H&E histopathology images**
- **Multiplexed IF images**
- **Spatial proteomics**
- **Spatial 3D genomics**
- …

**Scan here to download or learn more**



For Research Use Only. Not for use in diagnostic procedures.

Innovation with Integrity

# Cell Segmentation for Complex Neural Cell Morphologies & CosMx® Whole Transcriptomics Brain Imaging

**Lidan Wu, Aster Wardhani, Joseph-Tin Phan, Ashely Heck, Kimberly Young, Yi Cui, Stefan-Laural Rogers, Kathy Ton, Joseph Beechem**

Bruker Spatial Biology, Seattle, WA 98109, USA

## Abstract

Accurate cell segmentation is crucial for spatial omics, as incorrect cell boundaries can misassign transcripts or proteins, leading to skewed cellular profiles and flawed data interpretation. Brain tissue poses particular challenges due to its densely packed, irregularly shaped cells—many with star-like morphologies and long protrusions. Current machine-learning (ML) segmentation models often fail to capture these complex structures, as they are typically designed and trained on non-neuronal samples.

We present a novel cell segmentation pipeline designed for complex brain tissue morphology. The key innovations are a new neural-network model trained specifically for brain tissue and a custom post-processing method designed to recover large, irregular cells and their elongated structures, which are often missed by existing models. In validation using CosMx® data from FFPE human brain samples, we confirmed improved accuracy through both quantitative metrics and visual inspection.

## Methods

### Overview of cell segmentation pipeline

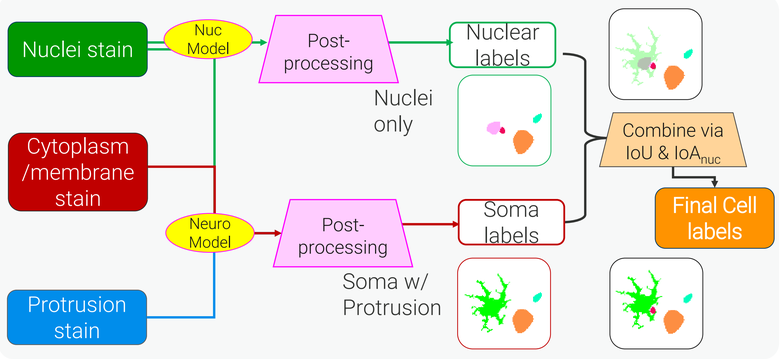


### 3-channel model for diverse neuro samples

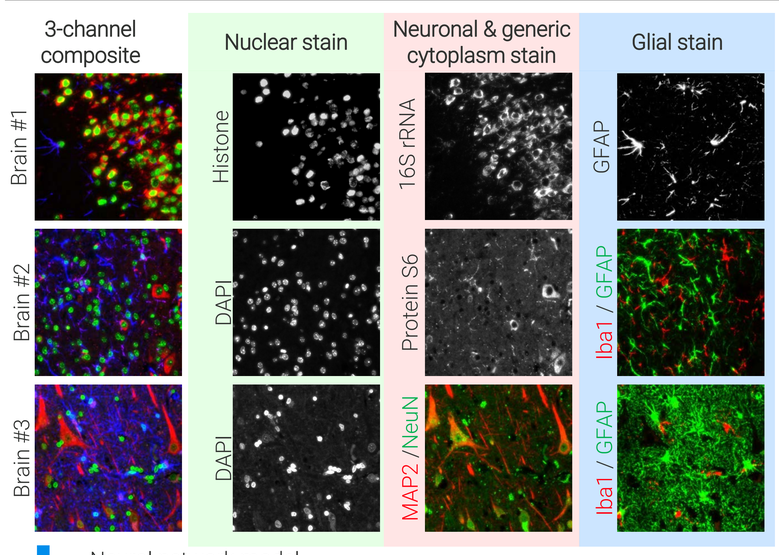


Neural network model (Cellpose ResNet architecture)

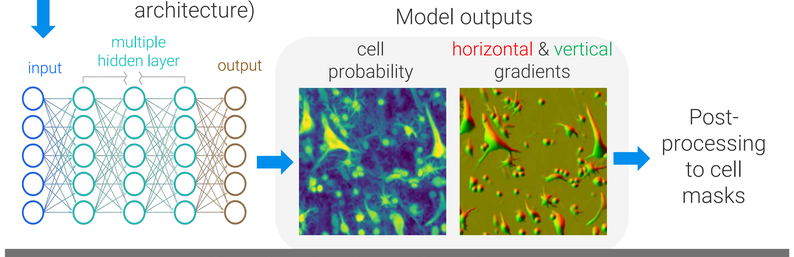


### Balanced training dataset from diverse sources

Carefully chosen ROIs for balanced representations of diverse morphological distinct cell types.

140 total neuronal images (128 3-channel + 12 single-stained)

16.5K total cells (16.3K 3-channel + 256 single-stained)

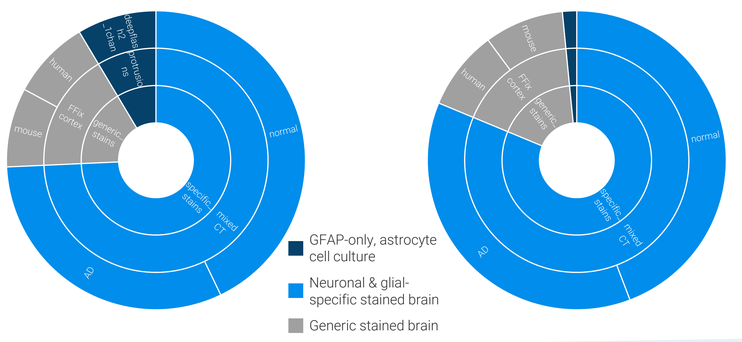


## Results

### Balanced representations increases model generalizability

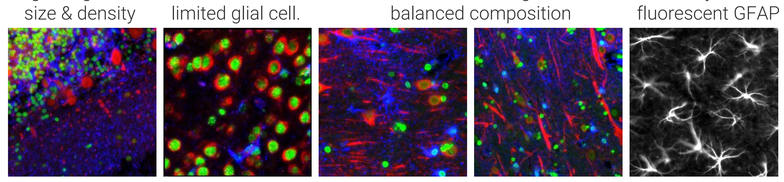


Diverse morphology from various parts of human and mouse brains are included in training.

- Roundish cells: main cell bodies stained with generic cytoplasm stain and/or nuclear stain.
- Single-positive nuclei with no obvious cytoplasm stain, very packed in cerebrum region.
- Star-like cells with protrusions: astrocytes, microglia, oligodendrocytes.
- Giant teardrop-like neurons +/- long protrusions: MAP2-positive neurons

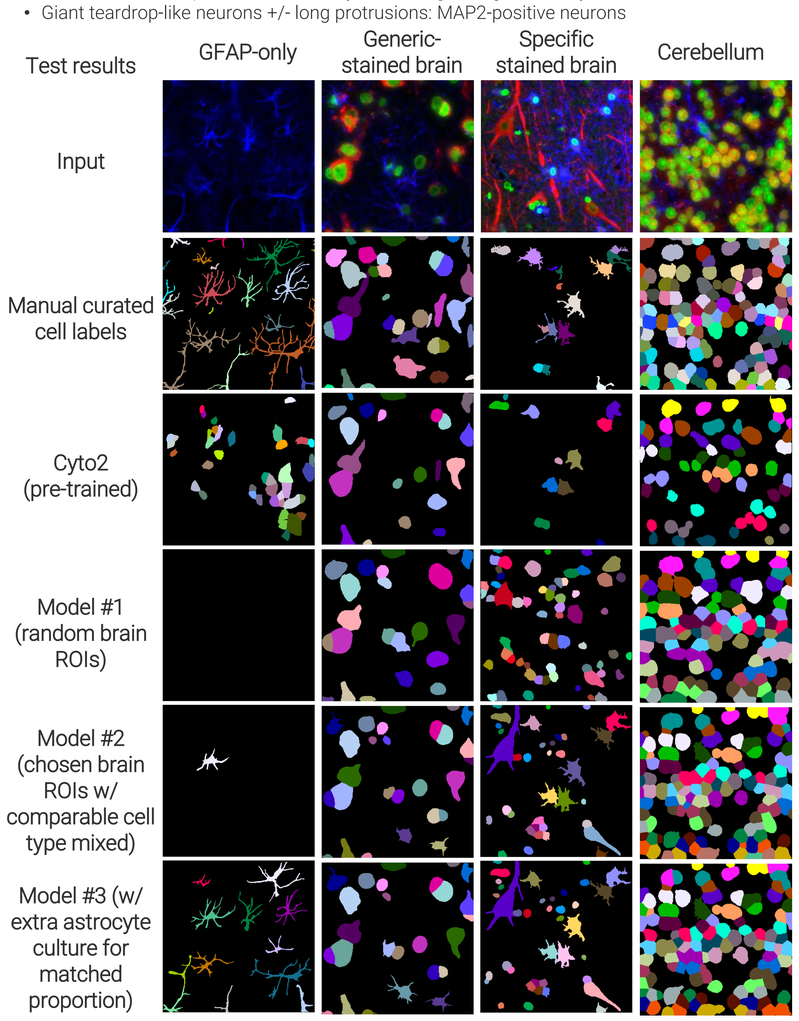


$$Sensitivity = \frac{TP}{TP + FN} \qquad Precision = \frac{TP}{TP + FP}$$

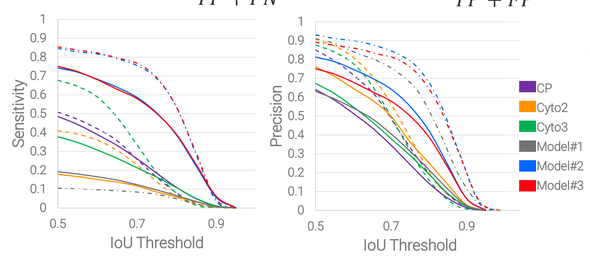


Solid lines: Diversified Test Set w/ Mixed Cell Types

Dashed lines: Cerebellum & Generic-stained Test Set

**Model #3** exhibited superior capacity in picking up fine protrusions while maintaining great performance across diverse datasets.

### Gradient tracking suffers for cells with elongated shape or of high texture

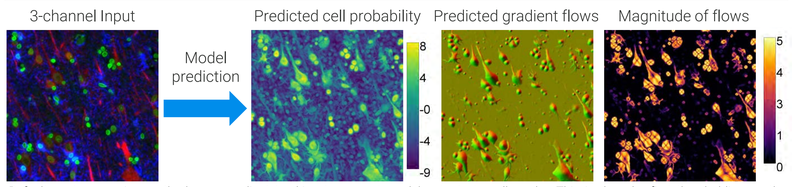


Default post-processing method uses gradient tracking to convert model outputs to cell marks. This is done by first thresholding on the predicted cell probability to isolate the foreground and then tracking the direction of the predicted flows given its magnitude in both horizontal and vertical directions to locate the basin point as cell centroid and connect pixels along the flow path as part of the corresponding cell.

Cells of elongated shape may have the centroid sitting outside of cell borders and thus result in negative divergence of flows at the nearest boundary pixel during gradient tracking, splitting cell marks into small pieces. Similarly, cells of high texture or large size tend to have less smooth flows predicted by a given cell segmentation model and thus are more susceptible to flow divergence and mask splitting. This issue can not be resolved by changing different thresholds on cell probability and/or flows.

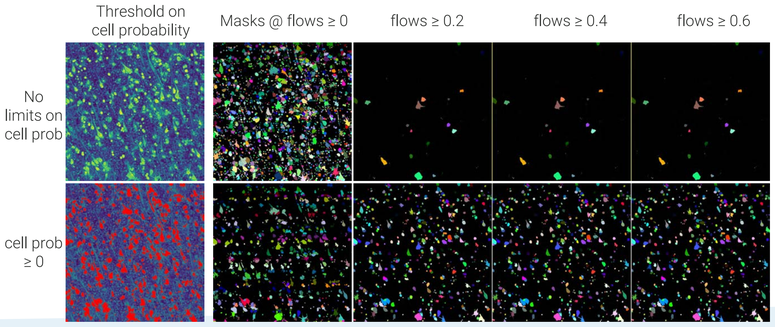


### High recovery post-processing for mask generation

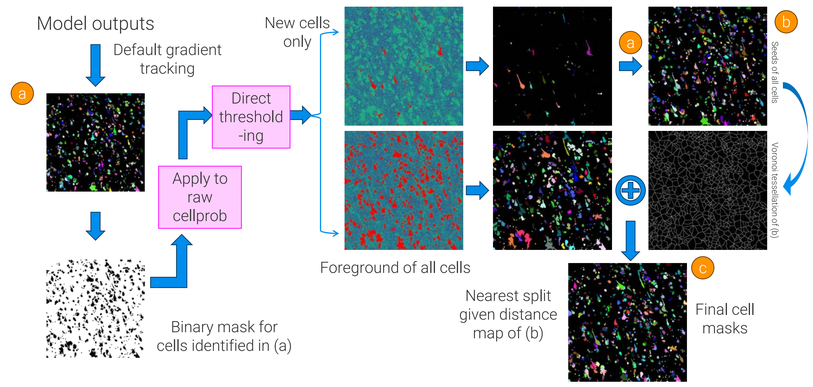


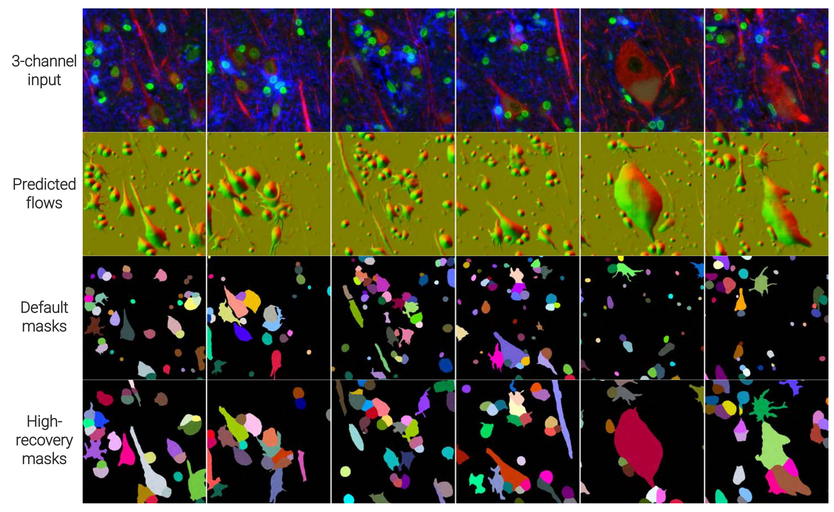


### New neuro cell segmentation improves quality of spatial transcriptomics data

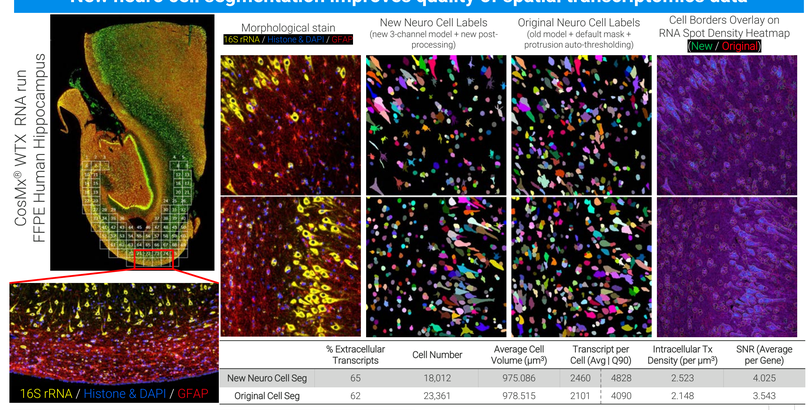


| | % Extracellular Transcripts | Cell Number | Average Cell Volume (µm³) | Transcript per Cell (Avg \| Q90) | | Intracellular Tx Density (per µm³) | SNR (Average per Gene) |
|---|---|---|---|---|---|---|---|
| New Neuro Cell Seg | 65 | 18,012 | 975.086 | 2460 | 4828 | 2.523 | 4.025 |
| Original Cell Seg | 62 | 23,361 | 978.515 | 2101 | 4090 | 2.148 | 3.543 |

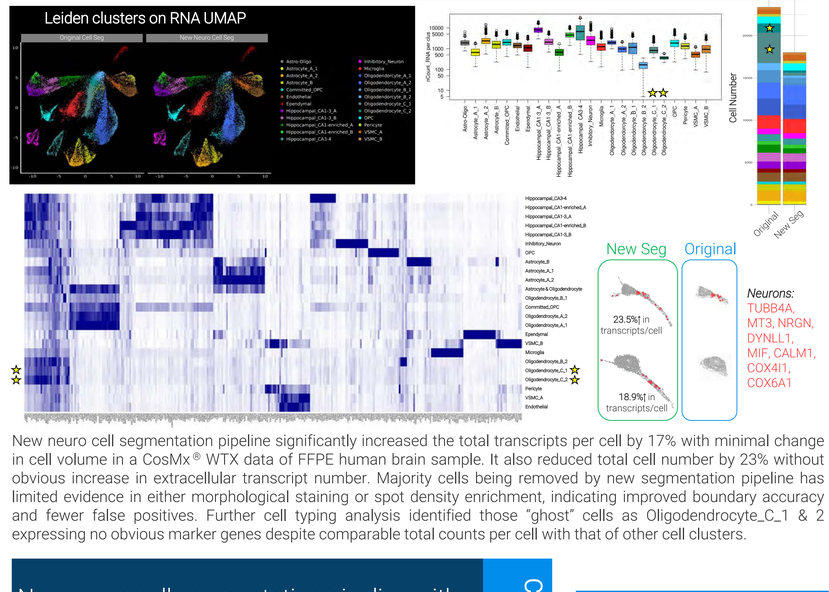


New neuro cell segmentation pipeline significantly increased the total transcripts per cell by 17% with minimal change in cell volume in a CosMx® WTX data of FFPE human brain sample. It also reduced total cell number by 23% without obvious increase in extracellular transcript number. Majority cells being removed by new segmentation pipeline has limited evidence in either morphological staining or spot density enrichment, indicating improved boundary accuracy and fewer false positives. Further cell typing analysis identified those "ghost" cells as Oligodendrocyte_C_1 & 2 expressing no obvious marker genes despite comparable total counts per cell with that of other cell clusters.

### New neuro cell segmentation pipeline with superior performance:

- Three color channels for better differentiation between closely positioned cells.
- Neuro-specific cell segmentation model with improved generalizability across diverse neuronal samples.
- High-recovery mask generation for large or elongated cells and better capture of long protrusions.
- Improved quality of spatial transcriptomics data

Cell Segmentation of CosMx® Spatial Molecular Imager

Scan here to download or learn more

# InSituDiff: Disease-driven changes in cellular neighborhoods as a window into spatial transcriptomics

**Patrick Danaher[1], Caleb Stokes[2,3], Dan McGuire[1], Lidan Wu[1], Parambir Dulai[4], Joseph M. Beechem[1]**

1. Bruker Spatial Biology, 2.University of Washington department of pediatrics, 3. Seattle Children's hospital division of pediatric infectious disease, 4. Division of Gastroenterology and Hepatology, Northwestern University

## Abstract

The fundamental problem in spatial transcriptomics: how do you find all the interesting biology hidden in your data?

InSituDiff pursues one solution: look for perturbed cellular neighborhoods in disease vs. control regions.

We transform the gene expression matrix into a "perturbation matrix".

Applied to this perturbation matrix, the usual arsenal of single cell analyses produces very revealing results.

## Algorithm: calculating perturbations in cellular neighborhoods

Record the expression profiles of all "cellular neighborhoods.




Match each cellular neighborhood in disease to the most similar control neighborhood.

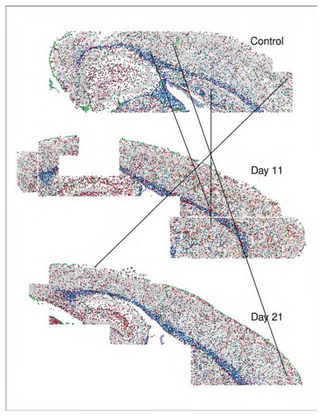


Record the differences from disease neighborhoods and matching control neighborhoods. This is the "perturbation matrix."

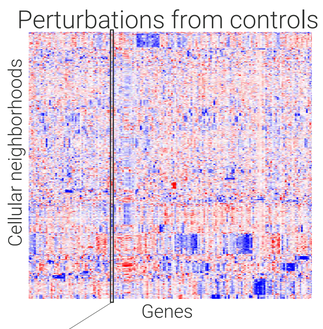


Perturbation scores from one gene

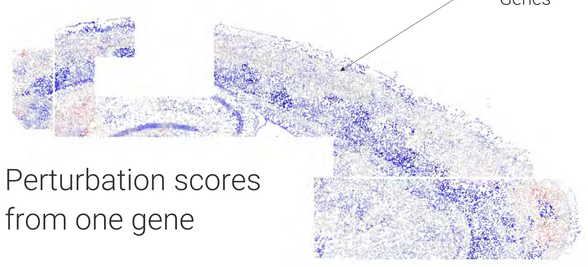

## Perturbation analysis of mouse brains after infection with West Nile Virus

Study: mouse brains, controls and 11 and 21 days post-infection with West Nile Virus, profiled with CosMx® Mouse Neuroscience Panel (1,000-plex).

### InSituDiff Application 1: identify highly-perturbed genes

Genes' total perturbations

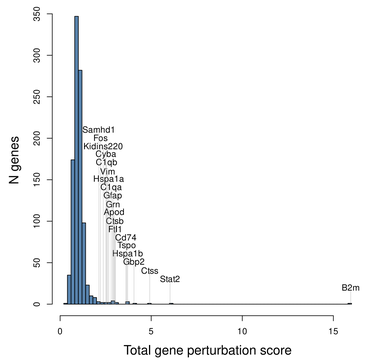


Role of individual cell types in genes' total perturbations

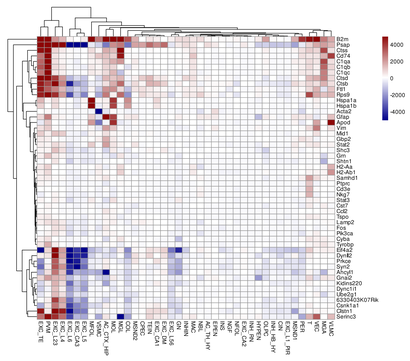

### InSituDiff Application 2: spatial correlation analysis of gene perturbations

Network of spatial correlations in gene perturbations

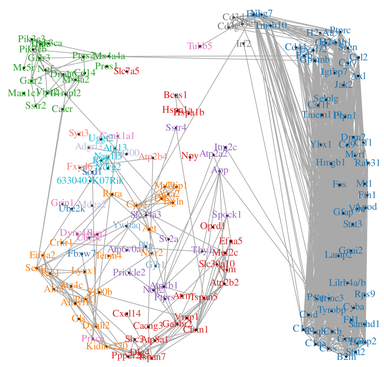

One module of genes with spatially-correlated perturbations

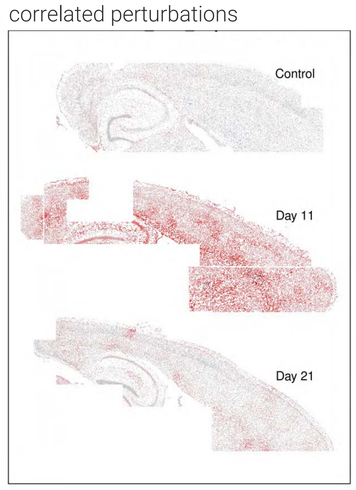


### InSituDiff Application 3: cluster cellular neighborhoods to discover spatial domains defined by perturbations

Four spatial domains derived from perturbation scores

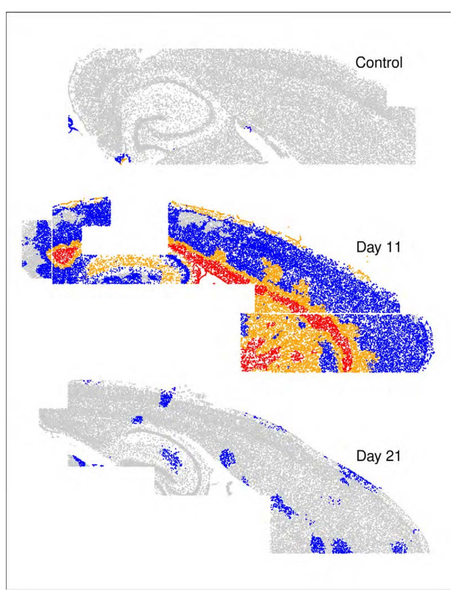


Mean gene perturbation values within domains

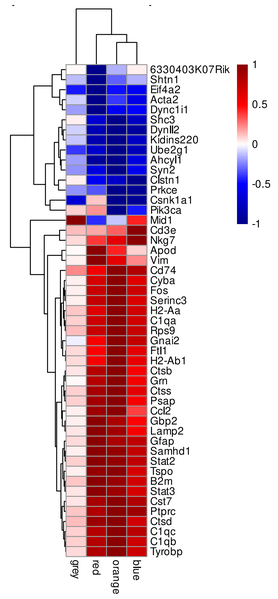


## Results from the CosMx whole transcriptome panel

Study: colon samples, one control and 3 IBD, profiled with the CosMx Human Whole Transcriptome Panel (18,933 genes)

478 highly perturbed genes clustered into 22 modules

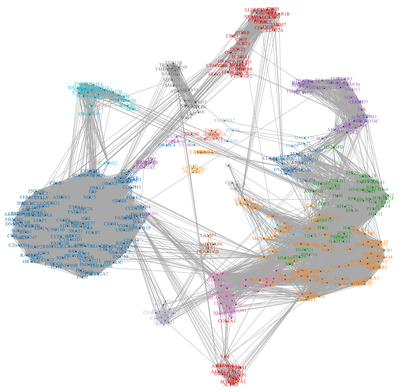

One highly perturbed gene: OR10H5: sensing of metabolites & inflammatory signals

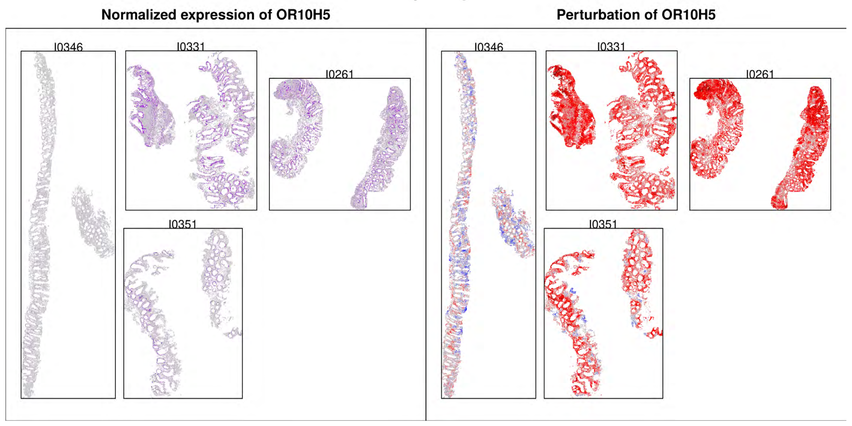


Spatial clustering identifies 6 perturbed spatial domains

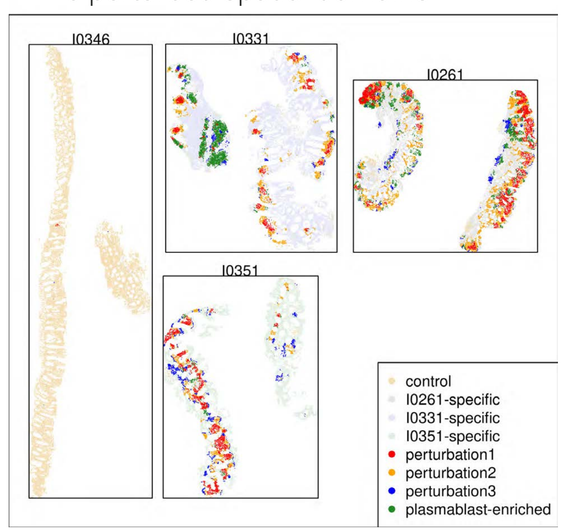


Mean perturbations in spatial domains

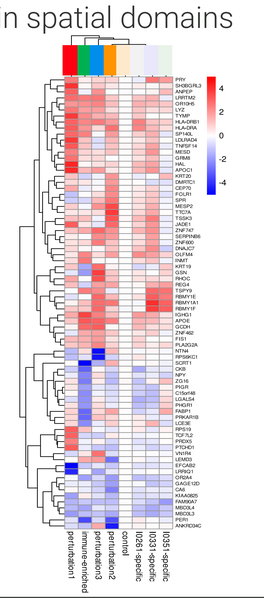


### Computational details

We limit memory and compute with subsetting and on-the-fly calculations

InSituDiff processed a 600k cell, 18k gene dataset in 11 minutes.

### Conclusion

We propose InSituDiff as a flexible and powerful tool for exploring spatial transcriptomics data.

**Scan here to read about InSituDiff on the CosMx Analysis Scratch Space**

**Scan here to Scan here to download or learn more**

# Connecting Form and Function: Mapping Microglial Spatial Biology in a Mouse Model of Acute and Chronic Ischemic Stroke


1. Bruker Spatial Biology, Seattle, WA

K. Young[1], A. Heck[1], A. Rosenbloom[1], A. Wardhani[1], M. Walter[1], R. Liu[1], L. Wu[1], C. Williams[1], M. Hoang[1], J. Beechem[1], K. P. Doyle[2], H. W. Morrison[3]

2. University of Arizona College of Medicine
3. University of Arizona College of Nursing


## Background

As the primary immune cells of the brain, microglia are extremely sensitive to changes in their environment, engaging in intricate communication networks that involve the exchange of small molecular signals that allow them to adapt their behavior based on a variety of stimuli in their vicinity.

These shifts in functional behavior, from surveillance to injury response, may be associated with morphological changes, which may serve as markers of their functional state.

To our knowledge, few have combined spatial proteomics and traditional immunohistochemistry (IHC) to map microglial form and function in situ following an ischemic stroke.

### Objective

**To use cutting-edge spatial biology tools to track microglial functional dynamics after ischemic stroke combined with a morphometric analysis at acute and chronic timepoints.**

## Methods

Following MCAO surgery, stroke severity was confirmed on a Bruker Biospec MRI scanner and comparable brains were selected for spatial proteomics profiling on the CosMx® Spatial Molecular Imager platform.

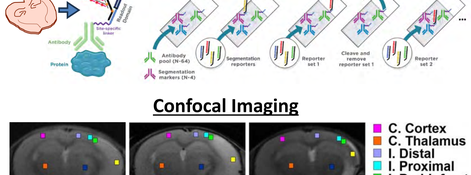

**Middle Cerebral Artery Occlusion (MCAO)** | **Bruker** Biospec 70/20 7.0T MRI scanner | CosMx SMI from Nanostring, a **Bruker** Company

### CosMx SMI Protein Assay Workflow


### Confocal Imaging

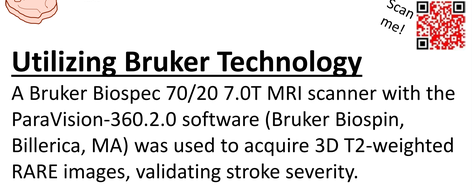


### Microglia Morphometrics

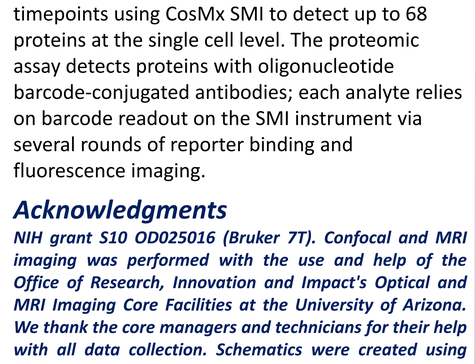


## Utilizing Bruker Technology

A Bruker Biospec 70/20 7.0T MRI scanner with the ParaVision-360.2.0 software (Bruker Biospin, Billerica, MA) was used to acquire 3D T2-weighted RARE images, validating stroke severity.

Proteomic data were collected within ROIs across timepoints using CosMx SMI to detect up to 68 proteins at the single cell level. The proteomic assay detects proteins with oligonucleotide barcode-conjugated antibodies; each analyte relies on barcode readout on the SMI instrument via several rounds of reporter binding and fluorescence imaging.


### *Acknowledgments*

***NIH grant S10 OD025016 (Bruker 7T). Confocal and MRI imaging was performed with the use and help of the Office of Research, Innovation and Impact's Optical and MRI Imaging Core Facilities at the University of Arizona. We thank the core managers and technicians for their help with all data collection. Schematics were created using BioRender.com.***


### *References*


Masuda T, Sankowski R, Staszewski O, Bottcher C, Amann L, Scheiwe C, et al. Spatial and temporal heterogeneity of mouse and human microglia at single-cell resolution. *Nature*. 2019;566:388-392

McCarthy MM. Location, location, location: Microglia are where they live. *Neuron*. 2017;95:233-235


## High-Plexity Reveals Microglial Morphology at 5 µm z-stacks

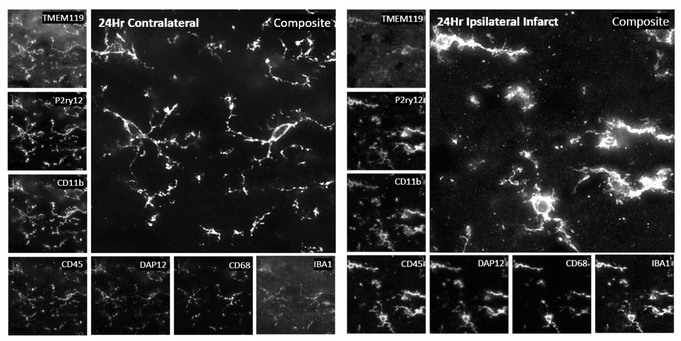


**Figure 1.** Multiple microglia/macrophage markers were included to create the composites used for skeleton analysis on CosMx images, capturing as much of the cell morphology as possible. Markers include both homeostatic and functional proteins.

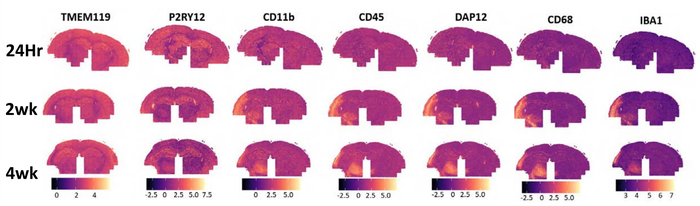


**Figure 2.** While spatial distribution of proteins like TMEM119 and P2RY12 remain relatively consistent across timepoints, intensity of proteins like DAP12 and CD68 becomes more localized to the infarct and scar regions at the 2wk and 4wk timepoints

## Microglia Morphometrics and Function

### Skeleton Analysis and Correlation Between 10 µm CosMx and 50 µm Confocal Images

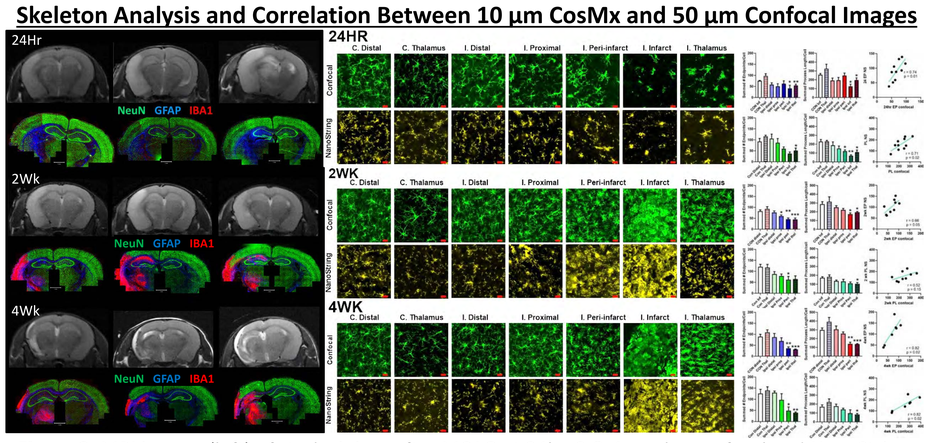


**Figure 3.** MRI images (left) of stroke injury after MCAO at 24hr, 2 & 4 weeks, confocal and NanoString images (middle) acquired in brain regions spatiotemporally related to stroke injury, and summary data of microglia morphology from confocal and NanoString Images. Animal n = 3; imaging sampling 2/region; data averaged per region for ANOVA analysis with post-hoc reported in figure: *p < 0.05, **p < 0.01, ***p < 0.001. Relationship between confocal and NanoString analysis carried out using Pearson's r.

### PCA Analysis of CosMx Microglia Proteins Identifies Region and Time-Point Variables

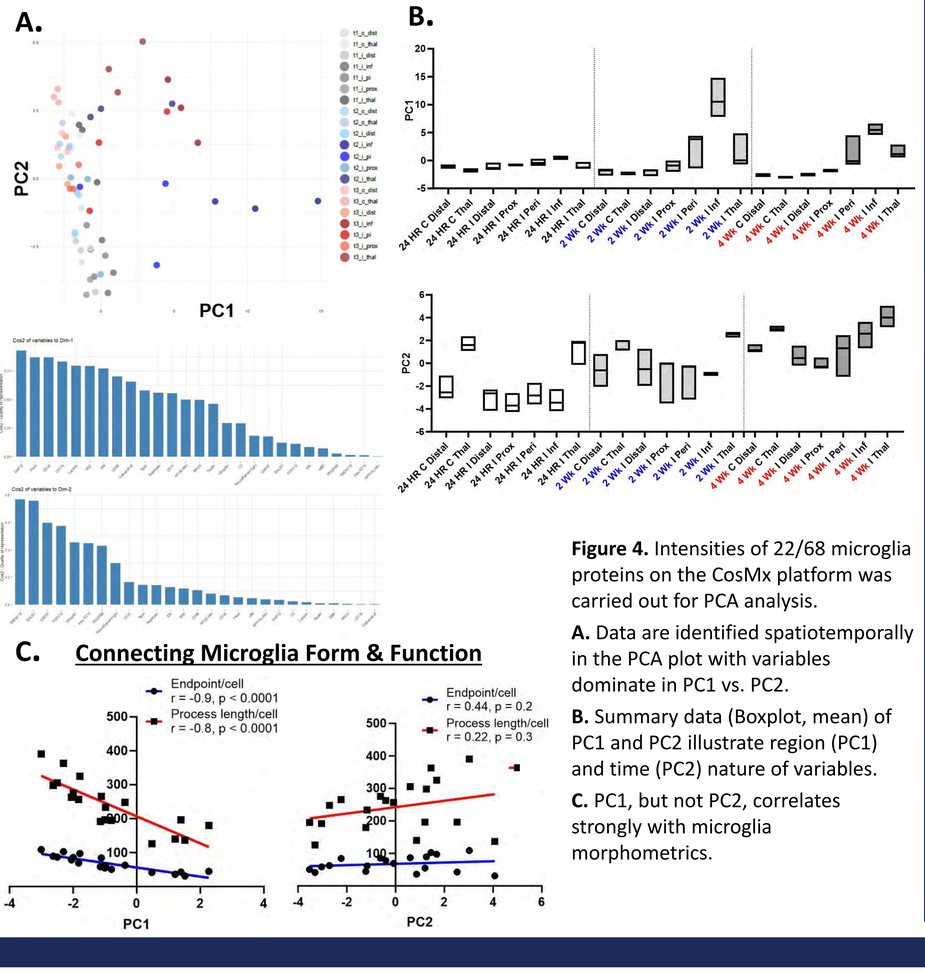


**Figure 4.** Intensities of 22/68 microglia proteins on the CosMx platform was carried out for PCA analysis.

**A.** Data are identified spatiotemporally in the PCA plot with variables dominate in PC1 vs. PC2.

**B.** Summary data (Boxplot, mean) of PC1 and PC2 illustrate region (PC1) and time (PC2) nature of variables.

**C.** PC1, but not PC2, correlates strongly with microglia morphometrics.

### C. Connecting Microglia Form & Function




## UMAPs and Unsupervised Leiden Clustering

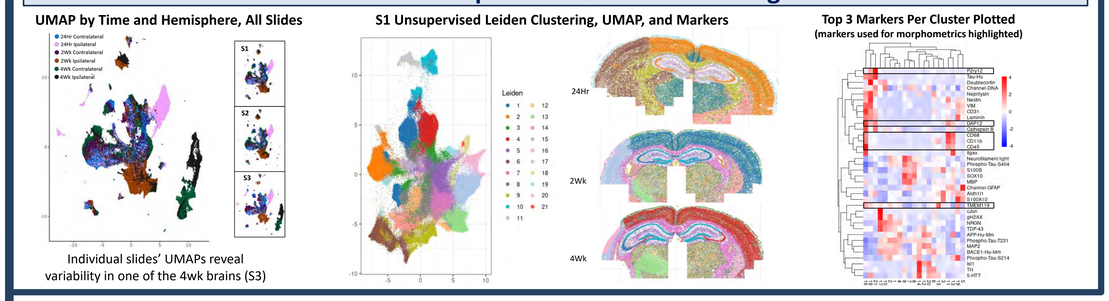


## InSituCor Identifies Spatially Correlated Proteins

### Clusters' Spatial Distribution, Marker Proteins, and Involvement Scores

**Figure 5.** InSituCor is an analysis toolkit that identifies spatially correlated proteins while considering cell type, signal strength, and background intensity.
**A.** Here, a module is highlighted in a 2wk post-stroke brain. Not all Leiden clusters are equally involved; cells in clusters 11 and 16 are equally likely to co-express the proteins identified in the module, while cells in cluster 13 are involved to a lesser extent.
**B.** An environment expression heatmap shows where protein correlation is strongest (yellow/bright) and weakest (purple/dark) in each of the sections.

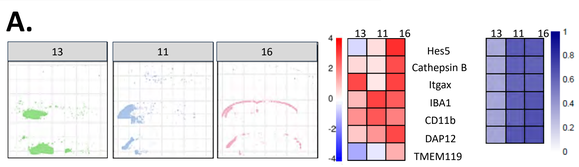


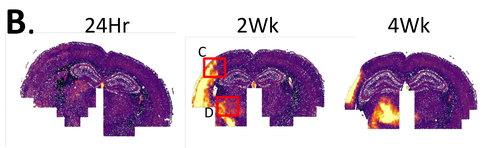


**C.** Among other proteins, this module includes the Notch pathway protein Hes5 (involved in cell differentiation), lysosomal enzyme Cathepsin B, and microglial/macrophage markers (IBA1, CD11b, Itgax) indicative of increased phagocytosis. Notably, the co-expression of each protein in the module changes with increasing distance from the infarct core. Hes5 intensity drops off at the peri-infarct region, and the number of Itgax+ and DAP12+ cells decreases.

At the proximal region, primarily IBA1 and CD11b remain, and DAP12 intensity sharply decreases. The fact that TMEM119, a microglia-specific protein, was not identified in this module may have implications for the identity of these cells. Alternatively, as the function of TMEM119 remains unknown, its absence from the module could inform investigations into its function.

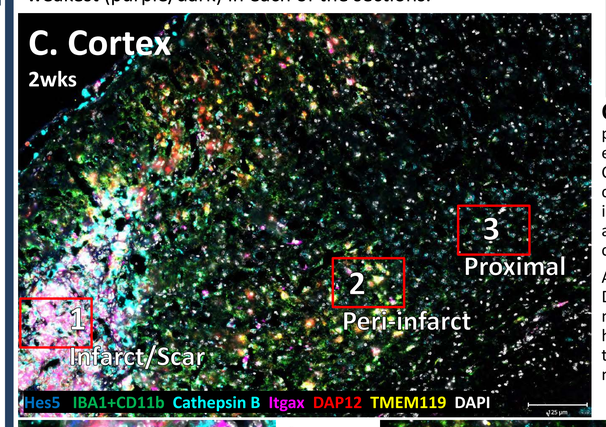


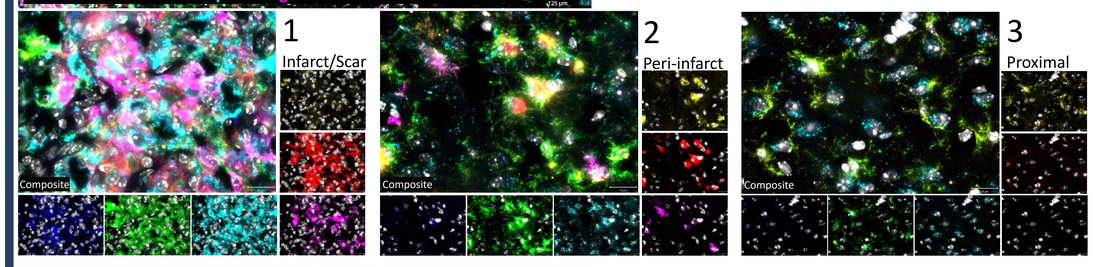


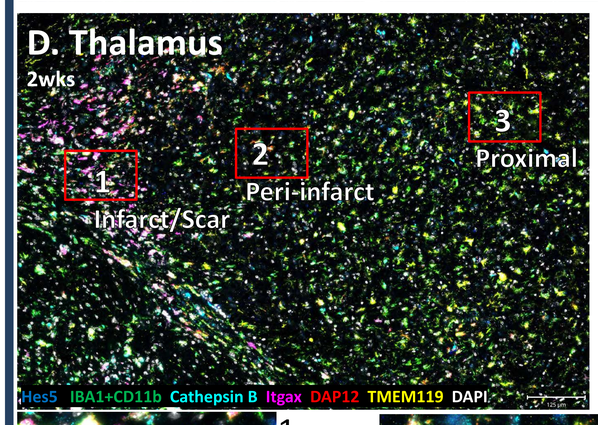


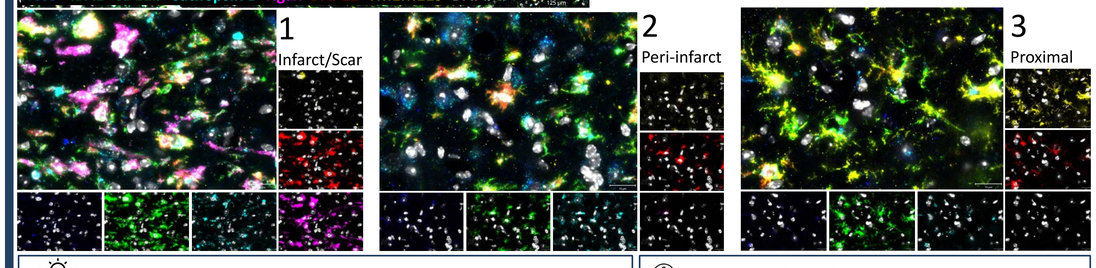


**D.** In the 2wk thalamus, Itgax expression appears largely restricted to the infarct core, with few Itgax+ cells visible in the peri-infarct region.

In addition, while cortical expression of DAP12 dropped off sharply at the proximal region, in the thalamus the number of DAP12+ cells appears similar between the peri-infarct and proximal regions, indicating that there may be a different cellular response in the cortex vs the thalamus.

Lastly, with increasing distance from the infarct core, the presence of TMEM119 increases more dramatically in the thalamus compared to the cortex. The difference in TMEM119 intensity across these two brain regions may have implications for the cell types involved; for example, the outer cortex regions may be more accessible to infiltrating macrophages (TMEM119-), whereas the degree of infiltration may be less significant in deeper midbrain regions like the thalamus.

## Conclusions

- Skeleton analysis of 10 µm multi-protein CosMx images correlates well with 50 µm IBA1 images. An initial analysis using only a subset of the 68 proteins detected reveals two distinct PCs: one that captures timepoint and another that captures brain region. PC1 correlates to microglia morphometrics.
- Combined UMAPs demonstrate minimal variability of replicates, and unsupervised leiden clustering reveals subtly distinct cell types and cell states across the contralateral cortex at each timepoint.
- InSituCor identifies spatially correlated proteins at the single-cell level, revealing a shift in the coexpression of IBA1, CD11b, Cathepsin B, Itgax, DAP12, and Hes5 with increasing distance from the infarct/scar at the 2- and 4-wk timepoints.

## Future Directions

**Improved Sensitivity With Next-Gen Cell Segmentation**

- While this preliminary study uses only IBA1 for microglia segmentation, implementing CosMx's improved cell segmentation would increase sensitivity by better capturing proteins expressed on fine microglial processes

**Composition of 4wk Glial Scar and Other Regions**

- The high-plexity of proteins captured in this study allows for a more in-depth investigation into additional players such as foam cells that exist within the 4wk glial scar, as well as considering changes in the hippocampus